

Mechanism and Substrate Recognition of Hydroxyethylphosphonate Dioxygenase

SUPPORTING INFORMATION

Spencer C. Peck^{1,2}, Heather A. Cooke^{1,2}, Robert M. Cicchillo², Petra Malova³, Friedrich Hammerschmidt³, Satish K. Nair⁴, and Wilfred A. van der Donk^{*,1,2}

¹Department of Chemistry and Howard Hughes Medical Institute,

²Institute for Genomic Biology

University of Illinois at Urbana-Champaign

1206 West Gregory Drive, Urbana, Illinois 61801

³Institute of Organic Chemistry, University of Vienna, Währingerstrasse 38, A-1090,
Vienna, Austria

⁴Department of Biochemistry and Center for Biophysics & Computational Biology

*Corresponding author: Tel. 217 244 5360; FAX: 217 244 8533; vddonk@illinois.edu

Supplemental Information:

Primer design. The mutated codon is in red.

K16A.

Forward: 5' tggatgaacgcccgccctacacggccgccagacc 3'

Reverse: 5' ggtctgggcggccgtgtaggcgcgggcgttcacagtgagc 3'

R90A.

Forward: 5' cgccgcccatccaggccgacggcatccacttc 3'

Reverse: 5' ggctggatggggcggcgggaggcgtcatctcc 3'

R90K.

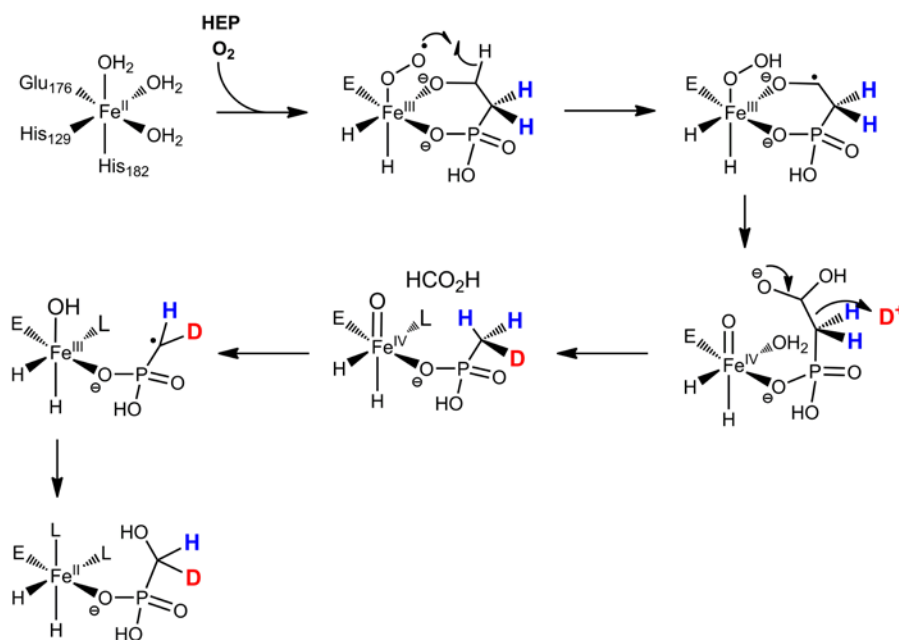
Forward: 5' cgccgcccatccagaaagacggcatccacttc 3'

Reverse: 5' ttctggatggggcggcgggaggcgtcatctcc 3'

Y98F.

Forward: 5' ggcattcacttctacaactacttcacgctcgccgcgccc 3'

Reverse: 5' gaagtgtgtagaagtggatgccctcgcgctg 3'



Scheme S1: An alternative mechanism involving a methylphosphonate intermediate that features hydroxylation of 2-HEP on C2, followed by C-C bond cleavage and protonation to generate methylphosphonate that could account for the observed racemization at C1. Subsequent hydroxylation of the methylphosphonate by the ferryl species would produce HMP. However, when carried out in D₂O, this pathway predicts incorporation of deuterium into the product HMP, which does not agree with the observed results

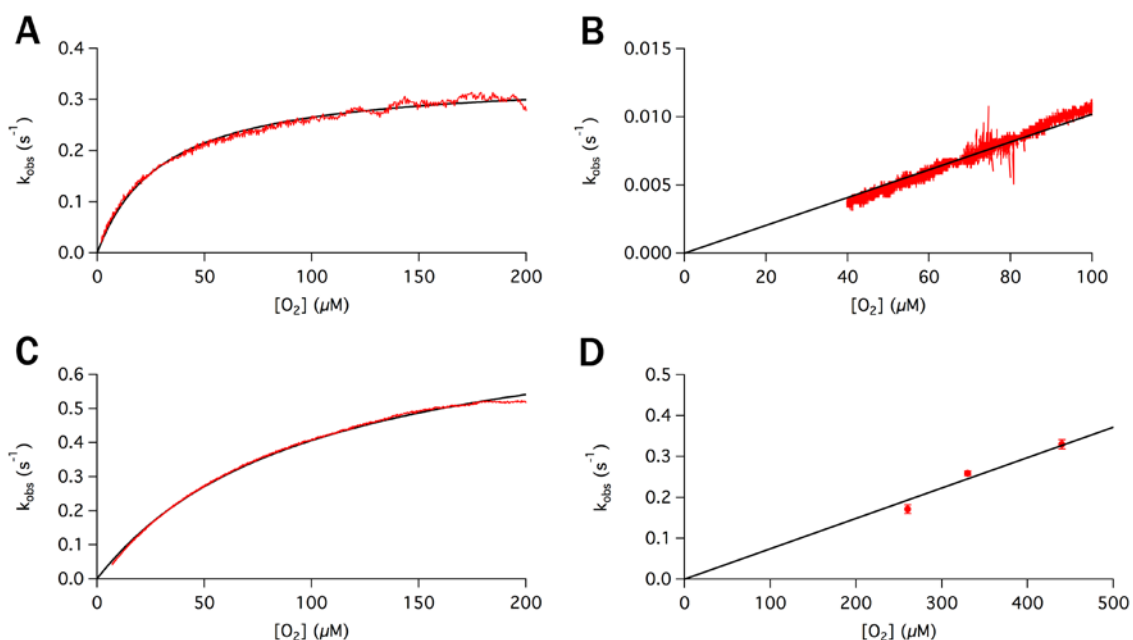


Figure S1: Oxidation kinetics with varying O_2 concentration for (A) wt HEPD, (B) R90A, (C) R90K, and (D) Y98F. In each case, the reaction was initiated with saturating concentrations of 2-HEP and then all O_2 was consumed to yield a plot of O_2 concentration as a function of time. At each O_2 concentration, a tangent line was constructed to give the near-continuous rate of O_2 consumption as a function of O_2 concentration (data in red). This data was then fit (black) to either a Michaelis-Menten curve (wt and R90K) or a line (R90A) for variants that could not be saturated. Not all O_2 was consumed in the case of R90A because the rate was too slow for accurate measurements below $40 \mu\text{M } O_2$. As noted in the main text, because Y98F undergoes gradual inactivation, the standard method of initial rates had to be used to obtain the rate of O_2 consumption as a function of O_2 concentration.

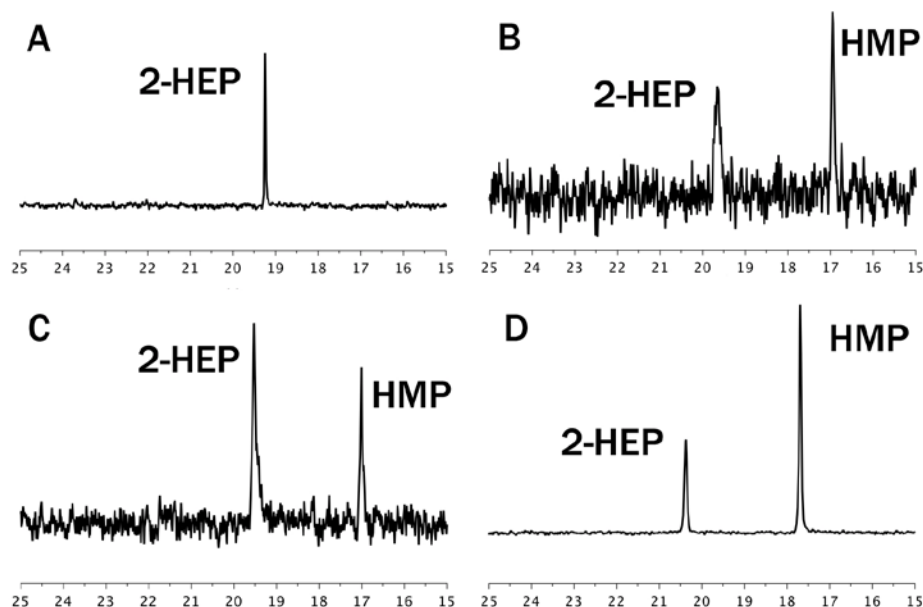


Figure S2: ^{31}P NMR spectroscopy was used to analyze reaction mixtures of 2-HEP with HEPD mutants (A) K16A (no reaction observed), (B) R90A, (C) R90K, and (D) Y98F. In all cases, HMP was the only product observable as confirmed by spiking with authentic material. (As noted in the main text, Y98F produces MPn as a side product at levels below the detection limits of ^{31}P NMR spectroscopy.)

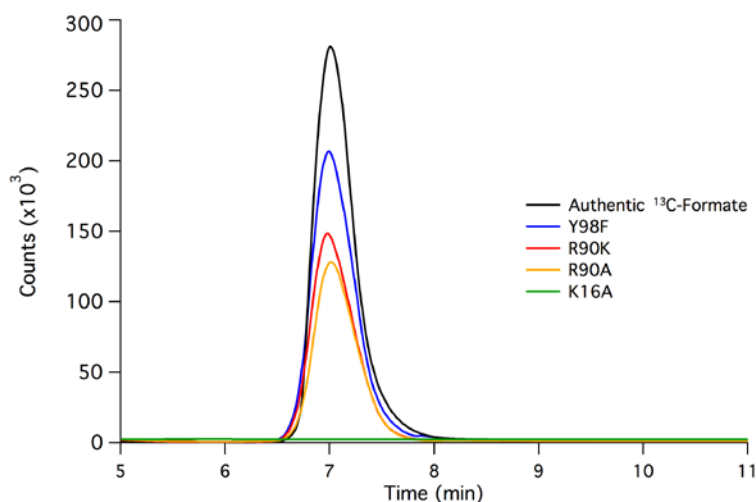


Figure S3: After incubating $[2-^{13}\text{C}_1]$ -2-HEP with the HEPD mutants, the organic acids were derivatized as previously described (1). LC-MS was used to confirm that derivatized ^{13}C -labeled formate ($m/z = 181$) was the second product of incubation of $[2-^{13}\text{C}_1]$ -2-HEP with HEPD mutants. Because the assays were quenched at different time points, the amount of ^{13}C formate present is not indicative of the rate of product formation. Quantitative rates were instead obtained with an oxygen electrode assay (Figure 3).

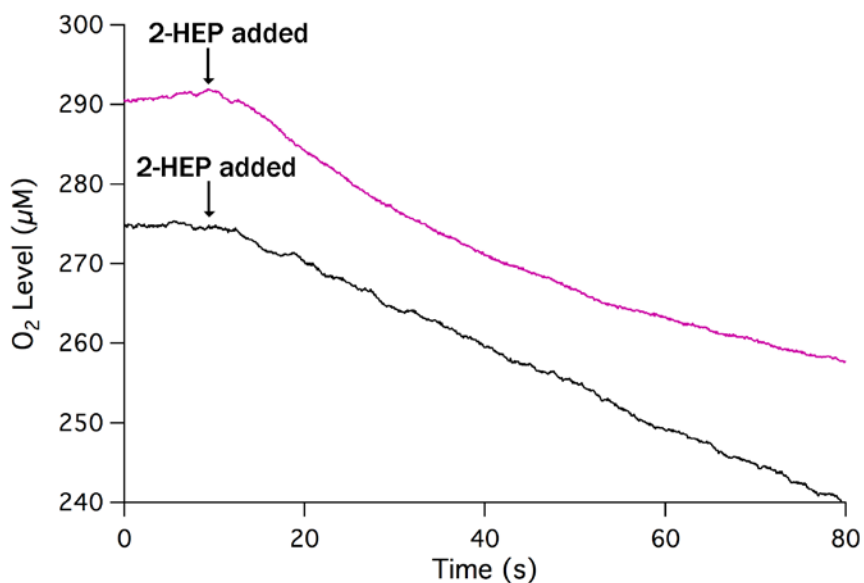


Figure S4: WT HEPD (black) steadily consumes O₂ whereas Y98F (purple) undergoes inactivation.

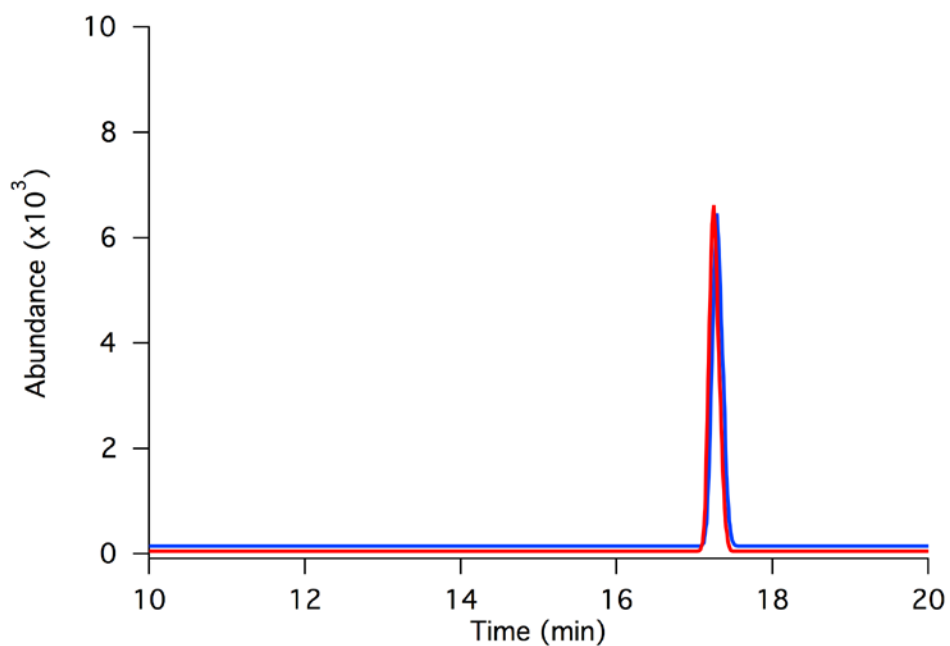


Figure S5: Extracted ion chromatograms of LC-FTMS analysis of the incubation of 2-HEP or 2-[1-¹³C₁]-HEP with Y98F led to the detection of MPn (red, found: 190.9877 *m/z*, calculated 190.9874 *m/z* for the noncovalent [MPn]₂⁻ dimer) and [¹³C₁]-MPn (blue, found: 192.9945 *m/z*, calculated 192.9941 *m/z* for the noncovalent [¹³C₁-MPn]₂⁻ dimer), respectively.

Table S1: Data collection and refinement statistics for HEPD mutant Y98F	
Space group	C222 ₁
Unit cell parameters (Å)	a=84.7,b=95.0,c=101.4
<i>Data collection</i>	
Resolution (Å)	50.0-2.20 (2.28-2.20)
Wavelength (Å)	1
No. of reflections (measured/unique)	111757/18990
% Completeness*	88.6 (62.2)
R _{merge} *	0.046 (0.277)
I/σ*	139.8 (17.9)
Redundancy*	5.9 (4.9)
<i>Refinement</i>	
No. of reflections (total/test)	17873/1757
R _{work}	0.207
R _{test}	0.268
No. amino acids	421
No. atoms	
Protein (chains A/B)	3230
Ligands (Cd)	15
Water Molecules	270
Mean B (protein/Cd/water)	41.9/63.9/47.2
r.m.s.d. from ideal geometry	
r.m.s.d bonds (Å)	0.005
r.m.s.d angles (°)	1.3
Ramachandran plot by PROCHECK (%)	
Core region	92.4
Allowed region	7.3
Generously allowed	0.3
Disallowed	0.0
PDB code	3RZZ

*overall (highest resolution shell)

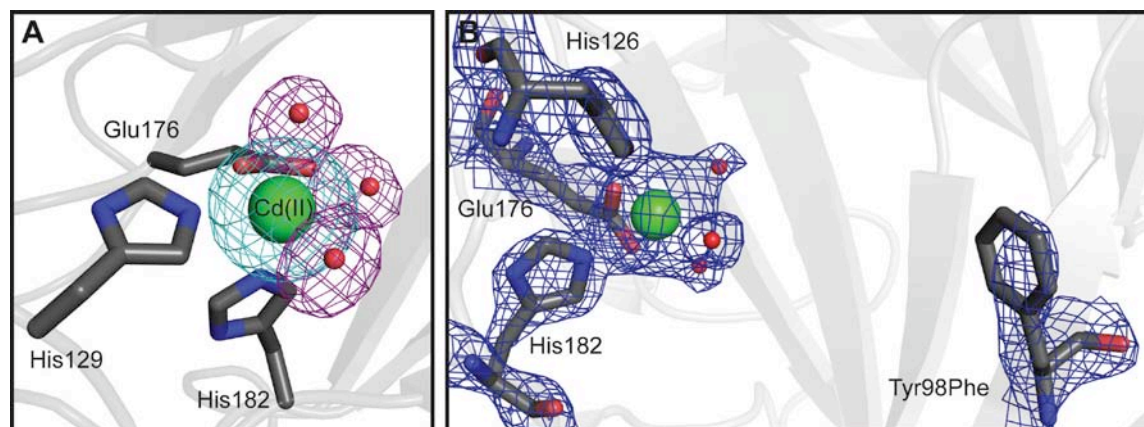


Figure S6: Electron density maps of the active site of the HEPD Y98F mutant. **(A)** Maps were calculated using model phases ($F_o - F_c$). The first map (contoured at 5 σ , in cyan) was calculated by omitting the cadmium ion (green sphere). The second map (contoured at 3 σ , in magenta) was calculated by omitting the metal-bound waters (red spheres). **(B)** Map ($2F_o - F_c$, contoured at 1.5 σ , in blue) was calculated for metal-ligands, metal bound waters, cadmium ion and Phe98. The incomplete density around Phe98 is likely due to the mobility of the residue in the active site.

References for SI:

1. Whitteck, J. T., Cicchillo, R. M., and van der Donk, W. A. (2009) Hydroperoxylation by Hydroxyethylphosphonate Dioxygenase, *J. Am. Chem. Soc.* *131*, 16225-16232.